

BBABIO 43125

## Excitation trapping efficiency and kinetics in *Rb. sphaeroides* R26.1 whole cells probed by photovoltage measurements on the picosecond time-scale

A. Dobek<sup>1,2</sup>, J. Deprez<sup>1</sup>, G. Paillotin<sup>1</sup>, W. Leibl<sup>3,\*</sup>, H.-W. Trissl<sup>3</sup> and J. Breton<sup>1</sup>

<sup>1</sup> Service de Biophysique, Département de Biologie, Centre d'Etudes Nucléaires de Saclay, Gif-sur-Yvette (France), <sup>2</sup> Institute of Physics, A. Mickiewicz University, Poznan (Poland), and <sup>3</sup> F.B. Biologie / Chemie, Biophysik, Universität Osnabrück, Osnabrück (F.R.G.)

(Received 23 May 1989)

(Revised manuscript received 19 September 1989)

Key words: Photosynthesis; Trapping; Exciton annihilation; Photovoltage; Purple bacterium; (*Rb. sphaeroides*)

Light-gradient photovoltage measurements in whole cells of the purple bacterium *Rb. sphaeroides* R26.1 were used to probe the trapping kinetics and the trapping efficiency resulting from 30 ps excitation at 532 nm. The time-course of the photovoltage is described by two distinct phases. The slower phase is characterized by a time constant of  $190 \pm 10$  ps, contributing to about 60% of the total amplitude. It is independent of the excitation energy and of the initial fraction of reaction centers (RC) in the open state (primary donor reduced). This phase is assigned to the forward electron transfer from the bacteriopheophytin intermediary acceptor to the quinone. The fast phase is assigned to the appearance of the primary charge separated state (i.e., trapping). If all the RCs were in the open state before excitation, the time constant of the fast phase decreased from  $55 \pm 10$  ps to less than 40 ps upon increasing the energy of the flash from less than 0.5 to more than 3 photons absorbed per RC. At the latter energy,  $90 \pm 5\%$  of the RCs are closed by the flash. If the initial concentration of RCs in the closed state was increased from 0 to about 100%, either by background illumination or by preexcitation with another picosecond flash delivered 20 ns before the measuring flash, the mean trapping time increased from  $55 \pm 10$  to  $90 \pm 15$  ps for a probe flash energy corresponding to 0.5 photon absorbed per RC. The data are analyzed and described in terms of the competition between trapping and exciton-exciton annihilation in the lake model of the photosynthetic membrane of purple bacteria (Deprez, J., Paillotin, G., Dobek, A., Leibl, W., Trissl, H.-W. and Breton, J. (1990) *Biochim. Biophys. Acta* 1015, 295–303).

### Introduction

The analysis of subnanosecond fluorescence lifetimes is the classical experimental approach to study migration, trapping and annihilation of excitons in the membrane of photosynthetic bacteria. In the case of *Rhodobacter sphaeroides*, *Rhodospirillum rubrum* or *Thiocapsa roseopersicina*, with open reaction centers (RC) a fluorescence decay time of  $60 \pm 10$  ps has been reported [1–3]. It increased to about 200 ps when the RCs are in the closed state characterized by an oxidized primary donor P [2,3]. In all cases, the fluorescence decay kinet-

ics, measured in the low energy limit, could be well fitted by single exponentials. When the RCs are in the open state before excitation, the lifetime of singlet excited bacteriochlorophyll antenna of *R. rubrum* chromatophores has been estimated to be  $60 \pm 15$  ps [4,5] and  $80 \pm 10$  ps [6] using picosecond absorption spectroscopy. It increased to 200–400 ps when the primary donor, P, was chemically oxidized [6].

Information about charge separation following the excitation of RCs of *Rb. sphaeroides* has been provided by picosecond and subpicosecond absorption change measurements in isolated RCs (for review see Ref. [7]). After formation of  $P^*$ , the excited state of the primary donor, charge separation between P and the bacteriopheophytin intermediary electron acceptor H ( $P^+H^-$ ), occurs in about 3 ps [8,9]. The subsequent electron transfer from H to the first stable quinone acceptor,  $Q_A$ , takes place in about 200 ps [7].

The different location of the primary electron car-

Abbreviations: RC, reaction center; PS, photosystem; PSU, photosynthetic unit.

\* Present address: CEN Saclay, France.

Correspondence: J. Breton, Service de Biophysique, Département de Biologie, CEN de Saclay, F-91191 Gif-sur-Yvette Cedex, France.

## List of terms used

$A_i$	electrogenicity factor
$\alpha$	parameter relating the competition between annihilation and trapping ( $\alpha = \gamma/2 \cdot \Gamma \cdot k_o$ )
$\Delta A_{820}$	absorption changes at 820 nm
$E_i$	energy of excitation flash (photons $\cdot \text{cm}^{-2}$ )
$f$	proportionality factor in the light-gradient theory
$\gamma$	bimolecular singlet-singlet annihilation rate constant
$\Gamma$	quantum yield of primary photosynthetic charge separation
$I_o$	intensity of dc-light (photons $\cdot \text{cm}^{-2} \cdot \text{s}^{-1}$ )
$k_i$	rate constants
$n(t)$	mean number of excitons per RC
$N$	antenna size/size of PSU (average number of antenna pigments per RC)
$q_o(t)$	fraction of open RCs
$Q_o$	fraction of open RCs before the flash
$q_{of}$	fraction of open RCs after the flash
$q_c(t)$	fraction of closed RCs
$\sigma$	absorption cross section of one mean antenna pigment
$T_{\text{eff}}$	transmission of one membrane of an effective vesicle
$\tau_i$	time constants
$V$	photovoltage
$V_o$	photovoltage created by closure of all RCs in a single membrane
$z$	normalized excitation in hits per trap ( $z = \sigma \cdot N \cdot E$ )

riers with respect to the membrane normal gives rise upon excitation to a transmembrane potential which can be monitored as a photovoltage in light-gradient experiments [10,11]. The amplitude of the photovoltage is correlated with the number of charge separations initiated by trapping of excitons at the RCs [12] and is proportional to the dielectrically weighted distance be-

tween the carriers involved in charge separation [13]. Thus, photovoltage measurements can provide information about the kinetics of trapping and of charge stabilization as well as about the yield and the electrogenicity of the primary events. This technique, developed in the nanosecond [10,13] and in the picosecond time-scales [11,14], has been proposed as an alternative approach to fluorescence lifetime or absorption change measurements. More specifically, exciton trapping and charge stabilization in *Rhodospseudomonas viridis* whole cells have been measured with picosecond resolution [14]. The photovoltage induced by a 30 ps laser flash gives rise to a biphasic increase in the photovoltage. The fast phase, contributing about 40–50% of the total amplitude, rises with a time constant no greater than 40 ps and is assigned to the trapping of the exciton at the RC. The slower phase,  $125 \pm 50$  ps, which disappears when the quinone is prereduced, is attributed to the forward electron transfer from H to  $Q_A$ .

In this study, three different types of photovoltage measurement are performed with *Rb. sphaeroides* R26.1 whole cells to probe the trapping time and the trapping efficiency for different redox states of the RCs: (i) single picosecond flash experiments, (ii) double picosecond flash experiments (actinic and probe flashes), (iii) continuous illumination during excitation by a picosecond flash. The data are analyzed in terms of the competition between trapping and exciton-exciton annihilation in the lake model [15] which has been shown to apply to the photosynthetic membrane of purple bacteria [16–19].

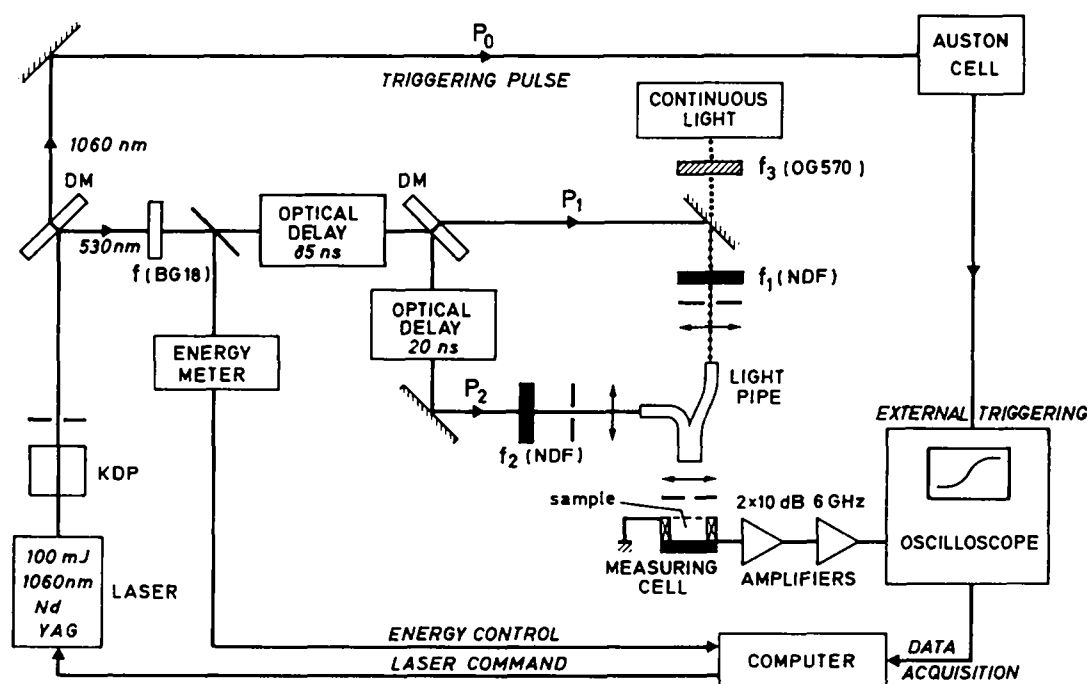


Fig. 1. Schematic diagram of the experimental apparatus. D.M., dichroic mirror; N.D.F., neutral density filter; BG18 and OG570, colored glass filters; KDP, frequency doubling crystal.

## Materials and Methods

*Rb. sphaeroides* R26.1 cells were grown as described in Ref. 20. For measurements, they were resuspended in Tris-HCl buffer (20 mM, pH 8) containing the electron mediator phenazine methosulfate (10  $\mu$ M), yielding an absorbance of 20 cm<sup>-1</sup> at 532 nm.

The electric measurements of the light gradient type were carried out essentially as described [11,14]. The measuring cell was built as a 3 mm diameter capacitor in a SMA-type micro-coaxial connector. The bottom electrode was a platinum disk and the top electrode was a platinum grid designed for electron microscopy [21]. The spacing between the two electrodes was 0.1 mm.

The apparatus is shown schematically in Fig. 1. The photovoltage signals were amplified with two cascaded 20 dB, 6 GHz amplifiers (Nucléide, France) and recorded as single sweeps on a 4 GHz oscilloscope (TSN 660.2, Thomson, France). The digitized single shot traces were subsequently stored in a computer for later signal analysis. Using a pulse generator (S50, Tektronix, USA) with a rise time of less than 25 ps, the 10% to 90% response time of the whole detection device was found to be 100 ps. The excitation source was a mode-locked Nd-YAG laser (YG-402, Quantel, France) delivering two simultaneous single 30 ps flashes at 1064 nm and 532 nm. The infrared one,  $P_0$ , was sent to an Auston photodiode [22] in order to trigger the oscilloscope. The 532 nm beam was divided into two flashes,  $P_1$  and  $P_2$ , by a beam splitter as shown in Fig. 1. The first flash  $P_1$  was sent directly to the sample, while the second one,  $P_2$ , entered a constant delay path of 20 ns. In single picosecond flash measurements, the  $P_1$  beam was blocked and the photovoltage signal elicited by  $P_2$  was recorded with or without background illumination. In double flash experiments,  $P_1$  served as an actinic pre-flash. An optical delay of 85 ns was introduced between the triggering flash  $P_0$  and the measuring flash  $P_2$  in order to compensate for the internal delay of the oscilloscope. Calibrated neutral density filters ( $f_1$  and  $f_2$ ) were utilized to vary the intensity of the flashes  $P_1$  and  $P_2$ . The flash energies were measured using an energy meter (RJ 7200, Laser Precision, USA) equipped with two detectors. This energy meter was used to calibrate the absolute energy at the location of the sample. For experiments in which continuous illumination was needed, the reflecting mirror directing the  $P_1$  flash to the sample was removed. The continuous light (Flexilux, Schöilly Fiberoptik, F.R.G.) was filtered by a 2-mm thick cutoff filter OG570 (Schott, F.R.G.) and sent to the sample along the same path as  $P_1$ . The flashes and continuous illumination were sent to the coaxial measuring cell via a bifurcated fiber-optic light guide. The emerging light was collected by means of a 20-D focusing lens and formed a 0.25 cm<sup>2</sup> homogeneous area on the entrance of the coaxial cell.

The experimental traces were compared with the results of a convolution calculation, assuming a biexponential charge displacement current and taking into account the response time of the experimental set-up, the duration of the laser flash and the time constant of the discharge of the measuring cell capacitance into the 50  $\Omega$  input impedance of the preamplifier [14,23]. The parameters of such fits are the time constants,  $\tau_1$  and  $\tau_2$ , of the two electrogenic phases of the photovoltage and the ratio  $A_2/A_1$  of the electrogenicity parameters that represent the change of the dipole strength associated with the two steps of charge transfer. Depending upon the signal-to-noise ratio of the data, this fitting procedure allows exponential risetimes longer than 30 to 40 ps to be determined.

For light-induced absorption change measurements at 820 nm ( $\Delta A_{820}$ ), the sample, prepared in the same way as for the photovoltage measurements, filled a rectangular 4  $\times$  1  $\times$  0.01-cm glass cuvette, which was placed at an angle of 45° to the analyzing 820 nm light beam. The continuous actinic light passed through the fiber-optic guide and illuminated the sample perpendicularly to the analyzing beam. The intensity of continuous illumination was adjusted with neutral density filters to the same levels as in the photovoltage measurements.

## Results

### Single picosecond flash excitation of dark-adapted bacteria

The time-course of the photovoltage elicited from whole cells of *Rb. sphaeroides* R26.1 by a single 30 ps flash is biphasic, as shown in Fig. 2, trace (a). As for the photovoltage traces obtained from *Rps. viridis* [14], the electrogenic reactions associated with these two phases are attributed to the primary charge separation between the primary donor, P, and the intermediary acceptor, H, and to the further electron transfer from H to the quinone  $Q_A$ .

In order to minimize the jitter effect due to the triggering circuit of the oscilloscope, a shift program was applied to recenter the individual traces on top of each other. In Fig. 2, ten single-shot traces resulting from successive laser flashes of an energy equal to  $(1.9 \pm 0.2) \cdot 10^{14}$  photons  $\cdot$  cm<sup>-2</sup> are superimposed (b). The kinetic trace (c) obtained by averaging these traces is shown in the lower part of Fig. 2, where the dashed line is calculated by assuming a biexponential displacement current (see Material and Methods). The best fit of curve (c) was obtained with the free running parameters  $\tau_1$ ,  $\tau_2$  and  $A_2/A_1$  yielding the values of 40 ps, 190 ps and 1.66, respectively.

The amplitude of the photovoltage increased with the energy of the flash as shown in Fig. 3a. Simultaneously the photovoltage rose faster. The results of the fit indicate that this acceleration is due to the shortening of the time constant  $\tau_1$  of the fast phase from  $55 \pm 10$  ps to

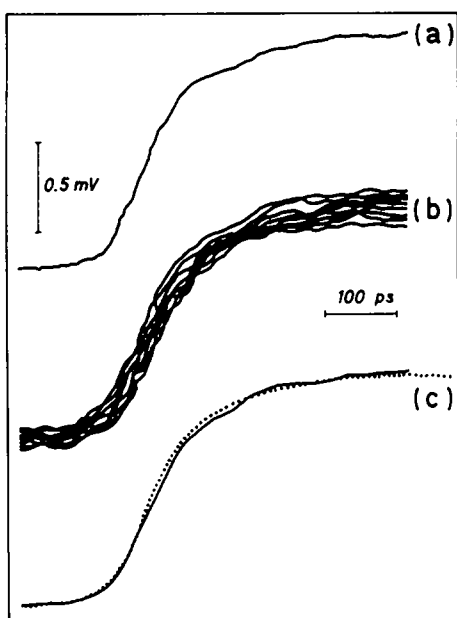


Fig. 2. Trace a: single sweep record of the photovoltage elicited by a 30 ps, 532 nm laser flash at an energy of  $1.9 \cdot 10^{14}$  photons  $\cdot$  cm $^{-2}$  from *Rb. sphaeroides* R26.1 whole cells. Traces b: ten single shot traces resulting from ten successive laser flashes at an energy of  $(1.9 \pm 0.2) \cdot 10^{14}$  photons  $\cdot$  cm $^{-2}$ , recentered and superimposed. Trace c: average of the ten traces corresponding to the individual sweeps depicted by traces b. The dashed line is calculated by assuming biexponential displacement current in the measuring cell.

$30 \pm 10$  ps when  $E$  increased from  $10^{13}$  to  $10^{15}$  photons  $\cdot$  cm $^{-2}$  (Fig. 3b). This indicates a faster trapping when the concentration of excitons is increased.

An increase of the excitation energy has little effect on the relative electrogenicity of the two phases ( $A_2/A_1 = 1.6 \pm 0.2$ ). As shown in Fig. 3b, the time constant  $\tau_2$  of the slower phase is equal to  $190 \pm 10$  ps in the whole range of excitation energy.

#### Single picosecond flash excitation with variable background illumination

The dependence of the photovoltage amplitude elicited by a 30 ps flash ( $E = 1.9 \cdot 10^{14}$  photons  $\cdot$  cm $^{-2}$ ) as a function of the intensity,  $I_0$ , of the 600 nm background illumination is depicted in Fig. 4a. This amplitude is normalized to the amplitude of the photovoltage recorded from dark-adapted bacteria with the same flash energy. In Fig. 4a the absorption changes,  $\Delta A_{820}$ , associated with the primary donor oxidation [24] are also plotted as a function of the intensity  $I_0$ .

The dependence of the time constant  $\tau_1$  of the fast electrogenic component on the background illumination intensity is shown in Fig. 4b. The increase of  $\tau_1$  from  $50 \pm 10$  ps for dark-adapted bacteria to  $90 \pm 15$  ps when  $P^+$  is accumulated by continuous light reflects a lengthening of the mean trapping time when the RCs are progressively closed before excitation. The 190 ps time constant of the slow phase and the ratio of the

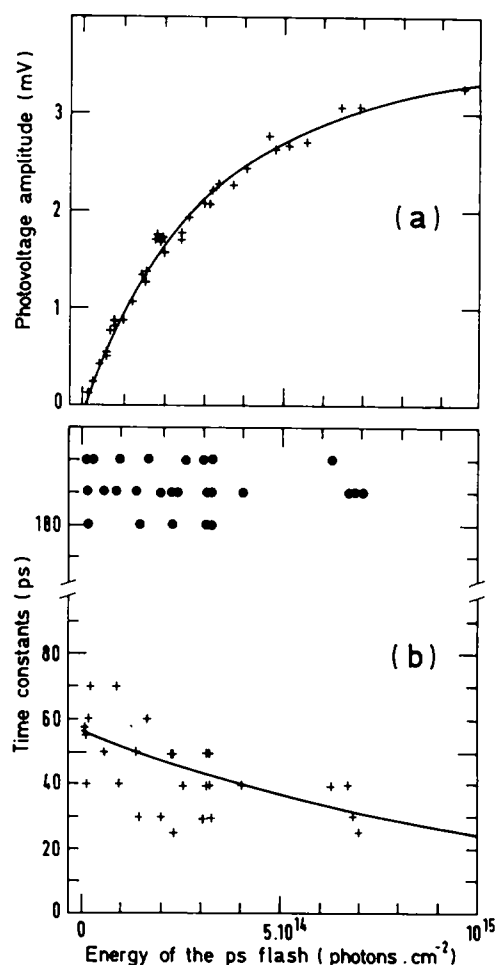


Fig. 3. (a) Amplitude of the photovoltage from *Rb. sphaeroides* R26.1 whole cells elicited by a 30 ps, 532 nm laser flash as a function of the excitation energy. (b) Time constants  $\tau_1$  (+) and  $\tau_2$  (●) of the fast and slow phases of the photovoltage as a function of the energy of the 30 ps, 532 nm excitation laser flash. Continuous lines in (a) and (b) result from calculations described in the text.

amplitude of the two phases were independent of the background light intensity. The latter observation shows that the state  $\text{PHQ}_A^-$  is not accumulated under the continuous illumination.

#### Double picosecond flash excitation

Fig. 4a shows that the amplitude of the photovoltage elicited from *Rb. sphaeroides* R26.1 by a picosecond flash of given energy can be used as a probe of the fraction of RCs oxidized before the flash. In order to characterize the efficiency of closure of the RCs by a picosecond flash, we have utilized pairs of picosecond flashes. The first flash,  $P_1$ , was used to close a fraction of the RCs, while the photovoltage signal induced by the second flash,  $P_2$ , incident at a time  $\Delta t = 20$  ns later was used to probe the RCs which were still open after the first flash. The delay time,  $\Delta t$ , was short enough to ensure that all the RCs which have trapped excitation created by  $P_1$  were still in the state  $P^+ \text{HQ}_A^-$  [18]. The

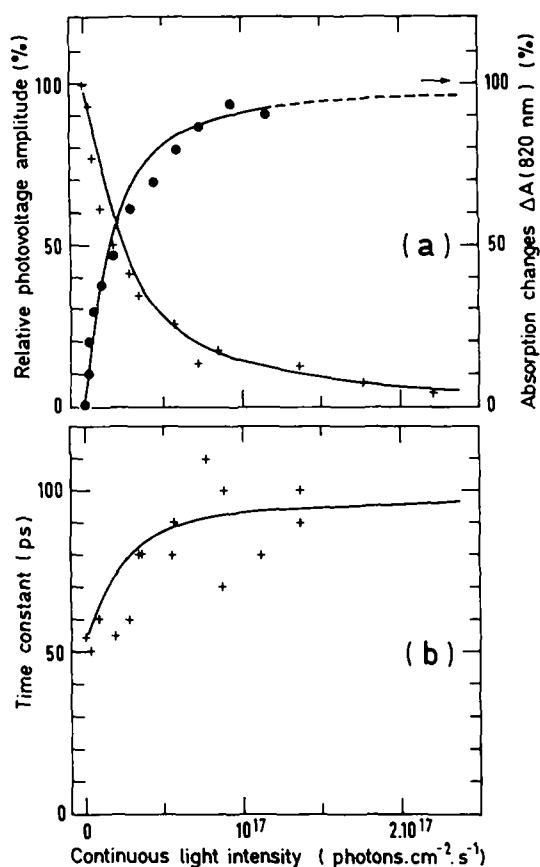


Fig. 4. (a) Absorption changes,  $\Delta A$ , induced at 820 nm in *Rb. sphaeroides* R26.1 whole cells by continuous illumination of variable intensity (●). Amplitude of the photovoltage elicited by a 30 ps, 532 nm laser flash,  $P_2$ , of constant energy ( $1.9 \cdot 10^{14}$  photons·cm<sup>-2</sup>) as a function of the intensity of the continuous illumination (+). The amplitude is normalized to the value measured with dark-adapted cells. (b) Time constant of the fast phase of the photovoltage induced by  $P_2$ . Calculated fits described in the text are drawn as continuous lines in (a) and (b).

energy of the probe flash  $P_2$  was held constant at  $1.9 \cdot 10^{14}$  photons·cm<sup>-2</sup>, while the energy  $E_1$  of the actinic flash  $P_1$  was varied.

The amplitude of the photovoltage created by  $P_2$ , normalized to the value obtained without  $P_1$ , is plotted as a function of  $E_1$  in Fig. 5a. The decrease of the photovoltage amplitude with increasing  $E_1$  is due to the progressive increase of the fraction of RCs closed by the actinic flash. The time constant  $\tau_1$  of the fast electrogenic component of the photovoltage induced by the probe flash  $P_2$  increased from  $55 \pm 10$  ps to  $90 \pm 10$  ps when the energy  $E_1$  increased from 0 to about  $1.6 \cdot 10^{15}$  photons·cm<sup>-2</sup> (Fig. 5b). As in the case of RCs closed by background illumination (Fig. 4b), this increase of  $\tau_1$  reflects an increase of the mean trapping time of the exciton created by the probe flash when the RCs are progressively closed.

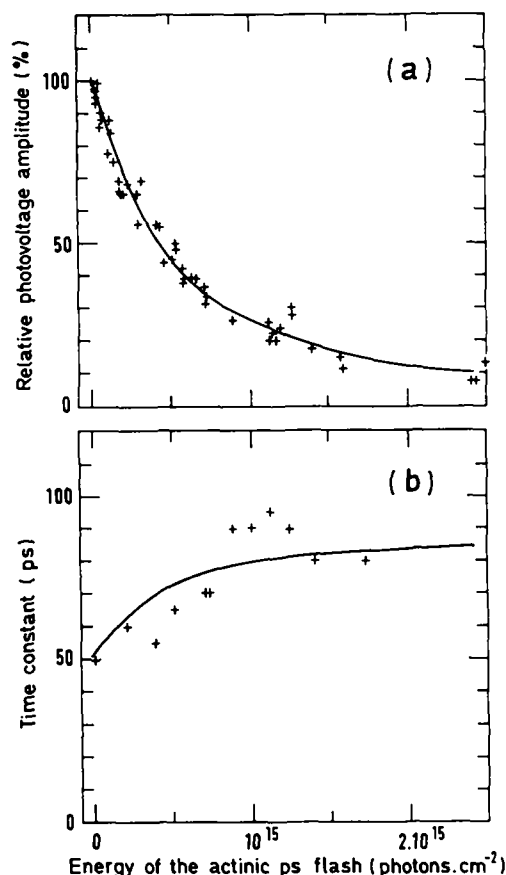


Fig. 5. (a) Amplitude of the photovoltage from *Rb. sphaeroides* R26.1 whole cells elicited by the 30 ps, 532 nm laser probe flash,  $P_2$ , of constant energy ( $1.9 \cdot 10^{14}$  photons·cm<sup>-2</sup>) as a function of the energy of the actinic flash,  $P_1$ . The amplitude is normalized to the value measured with dark-adapted cells in absence of  $P_1$ . The delay between  $P_2$  and  $P_1$  was 20 ns. (b) Time constant of the fast phase of the photovoltage induced by  $P_2$ . Calculated fits described in the text are drawn as continuous lines in (a) and (b).

## Data analysis

In Ref. 15, a macroscopic description of the exciton transfer and trapping in the photosynthetic membrane of purple bacteria is developed. It considers two states of the RCs during the lifetime of the excitons created by a picosecond flash: the open state  $\text{PHQ}_A$ , and the closed state in which the primary donor is oxidized ( $P^+$ ). They are distinguished by their different quenching rate constants,  $k_o$  and  $k_c$ , respectively. These rate constants include radiative and non-radiative losses in addition to quenching by the RCs. As in Ref. 15, we will denote by  $q_o$  and  $q_c$  the fractions of RCs in the open and closed states, respectively. The term  $\gamma$  is the bimolecular exciton-exciton annihilation rate constant,  $N$  is the average number of bacteriochlorophyll molecules per RC and  $\sigma$  is the mean absorption cross-section per molecule at the excitation wavelength. When the RCs are in the open state and when exciton-exciton annihilation is neglected (low energy limit),  $\Gamma$  is the

probability for an exciton to be irreversibly trapped by the RC, giving rise to the successive states  $P^+H^-Q_A$  and  $P^+HQ_A^-$ .

#### Estimation of the fraction of RCs closed by continuous illumination

The amplitude of the absorption change  $\Delta A_{820}$  as a function of the continuous light intensity,  $I_o$ , is proportional to the fraction,  $q_c$ , of oxidized primary donor,  $P^+$  [24]. Thus,

$$\Delta A = \Delta A_{\max} \cdot q_c = \Delta A_{\max} \cdot (1 - q_o) \quad (1)$$

For steady-state conditions, introducing  $k$ , the rate constant of regeneration of the open state,  $PHQ_A$ , from the closed state,  $P^+$ , Eqns. 5 and 6 in Ref. 15 can be rewritten:

$$\sigma \cdot N \cdot I_o - k_o \cdot n \cdot q_o - k_c \cdot n \cdot (1 - q_o) = 0 \quad (2)$$

$$k \cdot (1 - q_o) - \Gamma \cdot k_o \cdot n \cdot q_o = 0 \quad (3)$$

where  $n$  is the average number of excitons per RC. The normalized absorption change,  $\Delta A / \Delta A_{\max}$ , is related to the intensity,  $I_o$ , of the continuous light by Eqn. 4 deduced from Eqns. 1, 2 and 3.

$$I_o = K \cdot \frac{\Delta A}{\Delta A_{\max}} \left( 1 + \frac{\frac{k_c}{k_o}}{\frac{\Delta A_{\max}}{\Delta A} - 1} \right) \quad (4)$$

in which  $K = k / (\sigma \cdot N \cdot \Gamma)$ . The curve fitting the filled circle data points in Fig. 4a is obtained from Eqn. 4 with  $K = 2.6 \cdot 10^{16} \text{ cm}^{-2} \cdot \text{s}^{-1}$  and  $k_o/k_c = 3.0$ .

#### Photovoltage amplitude

If  $Q_o$  and  $q_{of}$  are the fractions of RCs in the open state before and after excitation by a picosecond flash, the amplitude  $V$  of the photovoltage induced by this flash is related to the fraction  $(Q_o - q_{of})$  of RCs closed by the flash according to Eqns. 14 and 14a in Ref. 12 in which the two adjustable parameters,  $f \cdot V_o$  and  $T_{\text{eff}}$ , are involved. The average number,  $z$ , of excitons created by a flash is proportional to its energy,  $E$ , and to the average absorption cross-section,  $N \cdot \sigma$ , of a PSU:

$$z = N \cdot \sigma \cdot E \quad (5)$$

Using Eqn. 11 in Ref. 15 with  $N \cdot \sigma$ ,  $k_o$ ,  $k_o/k_c$ ,  $\alpha = \gamma / (2 \cdot \Gamma \cdot k_o)$  and  $\Gamma$  as parameters,  $q_{of}$ , calculated as a function of  $Q_o$  and  $E$ , can be compared with experimental data. Thus, by combining the light gradient theory [12] and that describing trapping in a lake model [15], the energy dependence of the measured amplitudes and kinetics of the photovoltage can be analyzed.

TABLE I

List of the parameters used in this work to fit the data (excitation wavelength: 532 nm)

$T_{\text{eff}}$	$\Gamma \cdot N \cdot \sigma$ ( $\text{cm}^2$ )	$f \cdot V_o$ (mV)	$k_o/k_c$	$A_2/A_1$	$\alpha$
0.003	$2.85 \cdot 10^{-15}$	4	$3.0 \pm 0.2$	$1.6 \pm 0.2$	$1.0 \pm 0.1$

In single flash experiments with dark-adapted samples ( $Q_o = 1$ ),  $V$  is calculated as a function of  $E$  (Fig. 3a). If continuous light (intensity  $I_o$ ) or actinic picosecond flashes (energy  $E_1$ ) are used to partially close the RCs, the remaining fraction of open RCs,  $Q_o$ , can be determined using either Eqns. 1 and 4 or Eqn. 11 in Ref. 15. The amplitude  $V$  of the photovoltage elicited by the probe flash can be calculated as a function of  $I_o$  or  $E_1$  (Figs. 4a and 5a). All the continuous lines in Figs. 3a, 4a and 5a result from simultaneous fits using  $K = 2.6 \cdot 10^{16} \text{ cm}^{-2} \cdot \text{s}^{-1}$  and the set of parameters given in Table I.

#### Fast phase kinetics

The kinetics of the fast phase of the photovoltage reflect the disappearance of the fraction of RCs in the open state,  $q_o$ . These kinetics are described by Eqn. 9 in Ref. 15. The calculated  $1/e$  decay times are compared to the exponential rise time,  $\tau_1$ , of the fast phase of the photovoltage. As explained above,  $Q_o$  is determined from the background light intensity,  $I_o$ , or from the energy,  $E_1$ , of the actinic picosecond flash. The lines drawn in Figs. 3b, 4b and 5b are obtained using the same set of parameters as those used to fit the amplitude of the photovoltage and a monomolecular decay rate constant of  $k_o = (55 \text{ ps})^{-1}$ .

#### Discussion

##### Competition between trapping and exciton annihilation

The amplitude of the photovoltage elicited by the picosecond probe flash depends on the initial fraction of RCs in the open state (Figs. 4a and 5a). Absorption change data in Fig. 4a allow the amplitude of the photovoltage to be correlated with  $Q_o$ . It is then possible to obtain from the amplitude of the photovoltage induced by the probe flash,  $P_2$ , in Fig. 5a the initial fraction of RCs in the open state before excitation by  $P_2$ , and thus to deduce the fraction of RC closed by the picosecond actinic flash,  $P_1$ . This fraction increases with the energy of  $P_1$  and reaches 90% at  $E_1 = 1.2 \cdot 10^{15} \text{ photons} \cdot \text{cm}^{-2}$ , corresponding to  $z = 3.6$  (Fig. 6).

Exciton-exciton annihilations have been previously utilized to probe the organization of the antenna in purple bacteria [16–18]. In Ref. 18, it was found that, even with the strongest flash used ( $z > 5$ ) only 65% of the RCs in *R. rubrum* and 80% of the RCs in *Rb.*

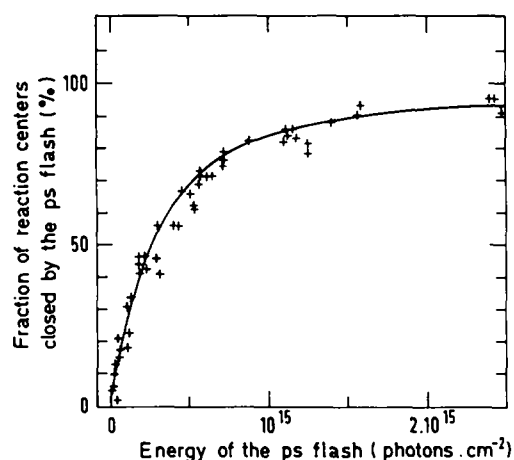


Fig. 6. Fraction of reaction centers of dark-adapted *Rb. sphaeroides* R26.1 whole cells closed by a 30 ps, 532 nm laser flash as a function of the excitation energy. The points are obtained by a comparison of the experimental data in Figs. 5a and 4a. The continuous line results from a fit described in the text.

*capsulatus* were oxidized. This relatively low efficiency of trapping, corresponding to a value of  $\alpha = 4$  in *R. rubrum* [15] reflects a severe competition between exciton-exciton annihilation and capture by the RCs. In contrast, the present results demonstrate a much weaker competition between exciton annihilation and trapping ( $\alpha = 1$ ) in *Rb. sphaeroides* R26.1. These differences in  $\alpha$  could be related to variations in the organization of peripheral and core antenna between the different organisms. Another factor which could play an important role is the presence of carotenoids which strongly absorb at the excitation wavelength of 532 nm in all the species investigated so far except the R26 and R26.1 mutants of *Rb. sphaeroides*. It has been shown that picosecond flash excitation at 532 nm of carotenoid-containing bacteria generates large amounts of carotenoid triplets via an exciton fission mechanism [25]. Such triplets, which are known to be efficient quenchers of singlet excitons, could thus cause severe competition between annihilation and trapping by RCs.

#### Dependence of the trapping efficiency on the initial fraction of RCs in the closed state

The relative amplitude of the photovoltage measured on the probe flash  $P_2$  as a function of the initial fraction ( $1 - Q_0$ ) of RC in the closed state is plotted in Fig. 7a. The continuous line is obtained from Eqn. 11 in Ref. 15 using the parameters deduced from Figs. 2 to 5. If all the PSUs were separated or if the quenching efficiencies of the RCs in the open and the closed states were the same ( $k_c = k_o$ ) [15,21,26], a linear relationship should be expected. The observed deviation from linearity is due to an increase of the apparent absorption cross-section of an open RC when the initial fraction of RCs in the closed state is increased [27].

#### The two components of the photovoltage signal

The time-course of the photovoltage signal measured in *Rb. sphaeroides* R26.1 whole cells demonstrates two distinct electrogenic events occurring during the first 500 ps as already observed in *Rps. viridis* [14]. Supposing a linear system, the photovoltage traces can be approximated by the convolution of the weighting function of the detection system and a biexponential displacement current (see Appendix in Ref. 14) with the time constant  $\tau_1$  (fast component) and  $\tau_2$  (slow component). The fast phase is associated with the kinetics of trapping, revealed by the charge separation between P and H [9], while the slower phase is attributed to the transfer of the electron from H to  $Q_A$ .

The ratio of the electrogenicities of these two reaction steps ( $1.6 \pm 0.2$ ) is independent of the energy of the exciting picosecond flash. X-ray crystallography models of the RC of *Rps. viridis* [28] and of *Rb. sphaeroides*

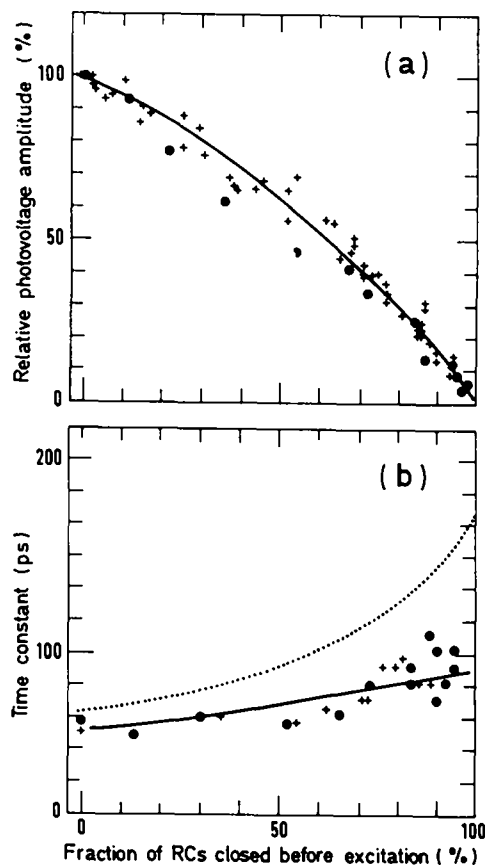


Fig. 7. (a) Amplitude of the photovoltage from *Rb. sphaeroides* R26.1 whole cells elicited by a 30 ps, 532 nm laser flash  $P_2$  of constant energy ( $1.9 \cdot 10^{14}$  photons  $\cdot$  cm $^{-2}$ ) as a function of the fraction of reaction centers closed before excitation either by background illumination ( $\bullet$ ) or by an actinic 30 ps, 532 nm laser flash ( $+$ ). The amplitude is normalized to the value measured when all the reaction centers are in the open state before excitation. (b) Time constant of the fast phase of the photovoltage induced by  $P_2$ . Calculated fits described in the text are drawn as continuous lines in (a) and (b). The dotted line in (b) is calculated in the low-energy limit (energy of  $P_2 < 10^{12}$  photons  $\cdot$  cm $^{-2}$ ) with the parameters given in Table I.

R26 [29,30] give a location of H in the middle between P and  $Q_A$ . The ratio  $A_2/A_1 = 1.6$  shows a higher dielectric constant of the protein environment between P and H than between H and  $Q_A$ . This agrees with analogous photovoltage measurements in *Rps. viridis* [14]. In comparison, the electrogenicity ratio of the charge transfer between the corresponding electron carrier molecules in the RC of PS II of higher plants is closer to unity [31,32]. The time constant,  $\tau_2 = 190 \pm 15$  ps, of the slower component is close to the time constant measured for the open state in isolated RCs of *Rb. sphaeroides* R26 for the reoxidation of  $H^-$  [7].

### Trapping kinetics of RCs in the open state

#### Dependence on the excitation energy

The time constant,  $\tau_1$ , of the fast component decreases upon increasing the flash energy (Fig. 3b). In principle, three phenomena may explain the decrease of the mean trapping time  $\tau_1$ . If the kinetics of trapping of the antenna excitation is a diffusion-limited process [33], the decrease of the mean diffusion length of the excitons in the antenna at higher energy gives rise to a faster excitation of the RCs. The shortening of the mean trapping time may be also observed in the trap-limited model [33] in which case the probability for an exciton to reside on the primary donor increases with the exciton density in the antenna. In addition, a further decrease in  $\tau_1$  is predicted for both models under conditions of exciton annihilation [34]. The present data do not allow a distinction between a trap-limited and a diffusion-limited model. In the present analysis, we have applied a model developed for the trap-limited case [15]. Within the framework of this model, a calculation of the energy dependence of the trapping time with and without annihilations (data not shown) indicates that, for a value of  $\alpha = 1$ , annihilation is not the dominant process which shortens the trapping time.

#### Dependence on the initial fraction of RCs in the closed state

As for the photovoltage amplitude analysis, the rise time of the fast phase of the photovoltage measured in the presence of continuous illumination (Fig. 4b) or after pre-excitation with an actinic picosecond flash (Fig. 5b) can be plotted as a function of the initial fraction ( $1-Q_0$ ) of RCs in the closed state (Fig. 7b). The trapping time constant increases from  $55 \pm 10$  to  $90 \pm 15$  ps when  $(1-Q_0)$  increases from 0 up to 1.

For the fluorescence decay measurements performed at low energy and when all the RCs are open, the kinetics of disappearance of the excitons in the antenna reflects the trapping kinetics. The time constants obtained from such fluorescence measurements [1–3] are close to the value  $\tau_1 = 55 \pm 10$  ps attributed to the trapping time in the present photovoltage measurements

(Fig. 3b). The value is also close to the lifetime of singlet excited bacteriochlorophyll in the antenna of purple bacteria chromatophores obtained from picosecond absorption spectroscopy [4–6].

Closing the RCs, the mean trapping time of the remaining open RCs, measured by photovoltage measurements increases up to  $90 \pm 15$  ps (Fig. 7b), whereas the exciton lifetime probed by fluorescence decay [2,3] or absorption change measurements [4,6] increases to more than 200 ps. The intensity of the probe flash used to record the risetime of the photovoltage in Figs. 4b, 5b and 7b corresponds to the closure of about 40% of the RCs when  $Q_0 = 1$  (Fig. 6), which is not in the low energy range. This explains the difference between the kinetics of the photovoltage and fluorescence measured for large fractions of closed RCs [2,3]. Nevertheless the theory developed in [15] together with the numerical value of the parameters deduced from this experimental work allows the trapping time in the low energy limit to be calculated (Fig. 7b). In *Rb. sphaeroides* R26.1 whole cells, the values of 60 and 190 ps determined from the present photovoltage measurements, cannot be easily reconciled with the 300 ps fluorescence decay reported in Ref. 17 for chromatophores of *Rb. sphaeroides* R26. Because of the difference between the strains of *Rb. sphaeroides* investigated and because the fluorescence lifetime measurements were performed with a streak camera under high-energy picosecond flash excitation, further analysis of this discrepancy should await new fluorescence results taken under low excitation conditions. On the other hand the trapping time values for open and closed RCs determined by photovoltage are in excellent agreement with those measured by fluorescence and absorption changes in the low energy limit but with different purple bacteria. Fluorescence and absorption change data on a variety of wild-type strains of purple bacteria [1–6,18] which differ by the organization of their antenna, have already demonstrated the homogeneity of the trapping kinetics by open or closed RCs in the low energy limit for all these organisms. Our photovoltage data further show that this homogeneity also extends to a carotenoid-deficient strain.

The increase in the mean exciton lifetime, probed by fluorescence measurements, is due essentially to the different quenching rate constants,  $k_o$  and  $k_c$ , of the open and closed states of the RCs. The mean trapping time constant of open RCs, probed by photovoltage measurements, is related to the mean lifetime of the excitons, i.e., to the time when the excitons are available somewhere in the antenna to be trapped. This time is also dependent on the probability of these excitons reaching open RCs, i.e., on the possibility for an exciton created in a PSU where the RC is in the closed state to escape from this PSU and to reach a PSU where the RC is in the open state. The analysis of our photovoltage data allows a discrimination between the lake and the



puddle model. In both models, if  $k_c < k_o$ , the exciton lifetime (fluorescence decay time) is expected to increase upon closure of the RCs. In the puddle model, the photovoltage amplitude should be proportional to  $Q_o$  and its kinetics should be independent of  $Q_o$  and  $k_o/k_c$ . In contrast, in the lake model and in the low-energy limit the photovoltage amplitude is no longer proportional to  $Q_o$  and both trapping and fluorescence kinetics are described by the same rate constant, whatever is the fraction of open RCs (Eqn. 6 in Ref. 15). The close analogy between the lengthening of the exciton lifetime probed by fluorescence decay measurements [2,3] and of the trapping time determined in our photovoltage measurements is thus compelling evidence in favor of the lake model description of the antenna organization in *Rb. sphaeroides* R26.1.

### Acknowledgements

The work at A. Mickiewicz University was in part supported by Research Project Nr: RP.II.13.1.10 to A.D.; W.L. and H.-W.T. acknowledge the financial support of the Deutsche Forschungsgemeinschaft (SFB 171). We thank R. Burgei and P. Bouyer (Département de Physique Nucléaire, CEN Saclay) for their generous loan of the fast oscilloscope.

### References

- Sebban, P. and Moya, I. (1976) *Biochim. Biophys. Acta* 722, 436–442.
- Borisov, A.Yu., Freiberg, A.M., Godik, V.I., Rebane, K.K. and Timpmann, K.E. (1985) *Biochim. Biophys. Acta* 807, 221–229.
- Godik, V.I., Timpmann, K.E., Freiberg, A.M., Borisov, A.Yu and Rebane, K.K. (1985) *Dokl. Akad. Nauk. SSSR* 284, 494–496.
- Borisov, A.Yu., Gadonas, R.A., Danielus, R.V., Piskarskas, A.S. and Razjivin, A.P. (1982) *FEBS Lett.* 138, 25–28.
- Razjivin, A.P., Danielus, R.V., Gadonas, R.A., Borisov, A.Yu. and Piskarskas, A.S. (1982) *FEBS Lett.* 143, 40–44.
- Nuijs, A.M., Van Grondelle, R., Joppe, H.L.P., Van Bochove, A.C. and Duysens, L.N.M. (1985) *Biochim. Biophys. Acta* 810, 94–105.
- Kirmaier, C. and Holten, D. (1987) *Photosynth. Res.* 13, 225–260.
- Woodbury, N.W., Becker, M., Middendorf, D. and Parson, W.W. (1985) *Biochemistry* 24, 7516–7521.
- Martin, J.L., Breton, J., Hoff, A.J., Migus, A. and Antonetti, A. (1986) *Proc. Natl. Acad. Sci. USA* 83, 957–961.
- Trissl, H.-W., Kunze, U. and Junge, W. (1982) *Biochim. Biophys. Acta* 682, 364–377.
- Trissl, H.-W. and Kunze, U. (1985) *Biochim. Biophys. Acta* 806, 136–144.
- Leibl, W. and Trissl, H.-W. (1990) *Biochim. Biophys. Acta* (1990) 1015, 304–312.
- Trissl, H.-W. (1983) *Proc. Natl. Acad. Sci. USA* 80, 7173–7177.
- Deprez, J., Trissl, H.-W. and Breton, J. (1986) *Proc. Natl. Acad. Sci. USA* 83, 1699–1703.
- Deprez, J., Paillotin, G., Dobek, A., Leibl, W., Trissl, H.-W. and Breton, J. (1990) *Biochim. Biophys. Acta* 1015, 295–303.
- Monger, T.G. and Parson, W.W. (1977) *Biochim. Biophys. Acta* 460, 393–407.
- Campillo, A.J., Hyer, R.C., Monger, T.G., Parson, W.W., Shapiro, S.L. (1977) *Proc. Natl. Acad. Sci. USA* 74, 1997–2001.
- Bakker, J.C.G., Van Grondelle, R. and Den Hollander, W.T.F. (1983) *Biochim. Biophys. Acta* 725, 508–518.
- Holmes, N.G., Van Grondelle, R., Hoff, A.J. and Duysens, L.N.M. (1976) *FEBS Lett.* 70, 185–190.
- Cohen-Basire, G., Suström, W.R. and Stanier, R.Y. (1957) *Cell. Comp. Physiol.* 49, 25–68.
- Trissl, H.-W., Leibl, W., Deprez, J., Dobek, A. and Breton, J. (1987) *Biochim. Biophys. Acta* 893, 320–332.
- Auston, D.H. (1977) in *Topics in Applied Physics* (Shapiro, S.L., ed.), Vol. 18, pp. 186–190, Springer, Berlin.
- Deprez, J. (1986) Thesis, Université Paris Sud, Orsay.
- Verméglio, A., Breton, J., Paillotin, G. and Cogdell, R. (1978) *Biochim. Biophys. Acta* 501, 514–530.
- Kingma, H., Van Grondelle, R. and Duysens, L.N.M. (1985) *Biochim. Biophys. Acta* 808, 383–399.
- Ley, A.C. and Mauzerall, D.C. (1986) *Biochim. Biophys. Acta* 850, 234–248.
- Joliot, A. and Joliot, P. (1964) *C.R. Acad. Sci. Paris* 258, 4622–4625.
- Deisenhofer, J., Epp, O., Miki, K., Huber, R. and Michel, H. (1984) *J. Mol. Biol.* 180, 395–398.
- Chang, C.H., Tiede, D., Tang, J., Smith, U., Norris, J. and Schiffer, M. (1986) *FEBS Lett.* 205, 82–86.
- Allen, J.P., Feher, G., Yeates, T.O., Komiya, H. and Rees, D.C. (1987) *Proc. Natl. Acad. Sci. USA* 84, 5730–5734.
- Trissl, H.-W. and Leibl, W. (1989) *FEBS Lett.* 244, 85–88.
- Leibl, W., Breton, J., Deprez, J. and Trissl, H.-W. (1989) *Photosynth. Res.* 22, 257–275.
- Pearlstein, R.M. (1982) *Photochem. Photobiol.* 35, 835–844.
- Breton, J. and Geacintov, N.E. (1980) *Biochim. Biophys. Acta* 594, 1–32.